PHYSICAL REVIEW LETTERS

η Condensate of Fermionic Atom Pairs via Adiabatic State Preparation

A. Kantian, A. J. Daley, and P. Zoller

*Institute for Theoretical Physics, University of Innsbruck, A-6020 Innsbruck,
Austria Institute for Quantum Optics and Quantum Information of the Austrian Academy of Sciences, A-6020 Innsbruck, Austria*

We discuss how an η condensate, corresponding to an exact excited eigenstate of the Fermi-Hubbard model, can be produced with cold atoms in an optical lattice. Using time-dependent density matrix renormalization group methods, we analyze a state preparation scheme beginning from a band insulator state in an optical superlattice. This state can act as an important test case, both for adiabatic preparation methods and the implementation of the many-body Hamiltonian, and measurements on the final state can be used to help detect associated errors.

Experiments with cold atoms in optical lattices not only make possible the realization of many-body lattice Hamiltonians and their corresponding ground states [1,2] but also exhibit long coherence times. This opens the way to produce excited many-body states and consider the related quantum dynamics, as demonstrated by recent investigations of repulsively bound atom pairs [3,4]. A key question in this context is how to prepare specific excited states, especially those corresponding to interesting quantum phases. Here we show that exact excited eigenstates of the Fermi-Hubbard model, the η-condensates first discussed by Yang [5], can be realized in experiments by combining an adiabatic ramp beginning from an insulating state in an optical superlattice with a sudden switch in the interaction strength [see Fig. 1(a)]. These states exhibit long-range order in all dimensions and have been discussed in the context of high temperature superconductivity [6]. Moreover, these exact excited eigenstates provide an ideal test case to address outstanding questions for quantum simulation with cold atoms in optical lattices: (i) the use of adiabatic ramping processes in state preparation [7–9], and (ii) validation of the many-body Hamiltonian, by testing the properties of the final state.

Below we show that the state preparation process proceeds with high fidelities for realistic experimental size scales and parameters, even in the presence of imperfections and noise. We focus on the one-dimensional (1D) case, where time-dependent density matrix renormalization group methods [10] allow exact calculations for relevant experimental conditions. However, the properties of the η condensate are essentially identical in higher dimensions, and we expect that this switch and ramp scheme will work similarly in 2D and 3D. We also show that the superlattice scheme has strong advantages over alternative schemes involving the adiabatic opening of a harmonic trap [9]. We then discuss how errors in state preparation or implementation of the Hubbard Hamiltonian can be revealed and characterized in experiments via measurements made on the η condensate.

The target state of our switch and ramp process, the η condensate, is an exact excited eigenstate of the Fermi-Hubbard Hamiltonian ($\hbar = 1$) in D dimensions:

$$H_{\mathrm{FH}} = -J \sum_{\langle \mathbf{i}, \mathbf{j} \rangle, \sigma} c^{\dagger}_{\mathbf{i}, \sigma} c_{\mathbf{j}, \sigma} + U \sum_{\mathbf{i}} n_{\mathbf{i}, \uparrow} n_{\mathbf{i}, \downarrow}. \quad (1)$$

This Hamiltonian describes the dynamics of atoms in the lowest band of an optical lattice [1,11], with $c_{\mathbf{i}, \sigma}$ a fermionic annihilation operator for particles of spin $\sigma = \{\uparrow, \downarrow\}$ on lattice site $\mathbf{i} = (i_1 \ldots, i_D)$, J the tunneling amplitude, U the on-site interaction energy shift, and $n_{\mathbf{i}, \sigma} \equiv c^{\dagger}_{\mathbf{i}\sigma} c_{\mathbf{i}\sigma}$. The η condensate can be constructed via the operator $\eta^{\dagger} \equiv \sum_{\mathbf{i}} (-1)^{\sum_{d=1}^{D} i_d} c^{\dagger}_{\mathbf{i}, \uparrow} c^{\dagger}_{\mathbf{i}, \downarrow}$ first introduced by Yang, which has the property $[H_{\mathrm{FH}}, \eta^{\dagger}] = U \eta^{\dagger}$. The state $|\eta_N\rangle \sim (\eta^{\dagger})^N |\mathrm{vac}\rangle$ is an eigenstate of H_{FH} with energy NU for positive integer N. Below we focus on the case $U > 0$, where $|\eta_N\rangle$ is a condensate of N repulsively bound atom pairs [3]. In Fig. 1(b), we plot the eigenenergies of H_{FH} for one particle of each spin in 1D, as a function of the center-of-mass quasimomentum k. The single η pair corresponds
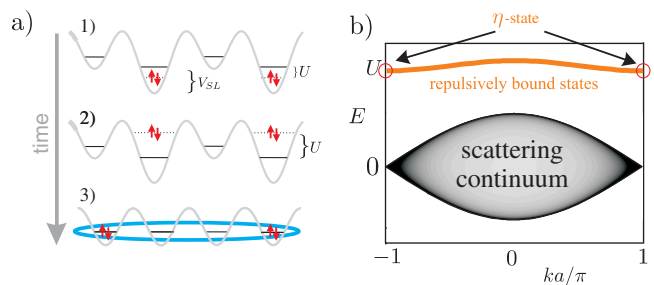

FIG. 1 (color online). (a) Preparation of an η condensate: (1) Begin in an insulator state $|\psi_i\rangle$ with attractive on-site interactions U in an optical superlattice with depth V_{SL}; (2) switch U to a positive value larger than the band gap; (3) delocalize on-site pairs by adiabatic removal of the superlattice. (b) Energy spectrum of H_{FH} with $U > 0$ in 1D for one atom of each spin species, plotted as a function of center-of-mass quasimomentum k, with a the lattice spacing.

to a repulsively bound on-site pair at the edge of the Brillouin zone, $k = \pi/a$.

Switch and ramp process.—The η condensate with N pairs can be prepared using a switch and ramp process, combining an adiabatic ramp with a sudden switch in the interaction strength. Adiabatic ramps have previously been discussed for preparation of many-body ground states in optical lattices [7,8]. In an adiabatic ramp, one prepares a state $|\psi_f\rangle$ of a Hamiltonian H_0 beginning from a non-degenerate, gapped initial state $|\psi_i\rangle$ that is an eigenstate of the Hamiltonian $H_0 + V$. By removing V adiabatically, the state follows the instantaneous eigenstates of $H_0 + V(t)$ and ends in $|\psi_f\rangle$. The key is that $|\psi_i\rangle$ should be a gapped state of $H_0 + V$ that can be prepared with low entropy via standard cooling and loading techniques [7,12].

Here we propose to begin from a band insulator in the lowest sites of an optical superlattice [13], as depicted on the left in Fig. 2(a), which is the ground state of $H_{\mathrm{FH}} + V$, with V the Hamiltonian describing the superlattice potential. For the case depicted in Figs. 1(a) and 2(a), where the superlattice period is twice the original lattice spacing, $V = V_{\mathrm{SL}}\sum_{i\,\mathrm{even}} n_i$. At this stage we require $U \ll V_{\mathrm{SL}}$, and we choose $U < 0$ in Fig. 2(a). This state has an energy gap $\epsilon_{\mathrm{SL}} \sim V_{\mathrm{SL}}$ corresponding to the superlattice band gap, and a filling factor which is set by the superlattice period [7] [e.g., half filling in Figs. 1(a) and 2(a)]. If we were to let $V_{\mathrm{SL}} \to 0$ adiabatically, we would connect this ground state to the ground state of H_{FH}. Instead, we can suddenly switch U (on a time scale short compared with J^{-1}) to a value larger than ϵ_{SL} [see Fig. 1(a)]. In the limit $|U - \epsilon_{\mathrm{SL}}| \gg J$, this switching will create an excited eigenstate of $H_{\mathrm{FH}} + V$, as shown in the transition from the left panel to the right

panel in Fig. 2(a). Adiabatic removal of the superlattice, $V_{\mathrm{SL}} \to 0$, will then lead to an excited eigenstate of H_{FH}. This latter state will correspond to the lowest energy state in which all particles exist in repulsively bound pairs, which is the η condensate. The energy spectrum of the Hamiltonian during the ramp is plotted in Fig. 2(a) for a small 1D system, and we see that the state is always separated by a gap $\sim U$ to lower lying states, and the gap from the superlattice $\sim V_{\mathrm{SL}}$. While, in general, the adiabatic ramp could be optimized using optimal control methods [14], we choose a simple exponential ramp for the superlattice, $V_{\mathrm{SL}}(t) = (e^{-t\nu} - e^{-\nu T})/(1 - e^{-\nu T})$, motivated by the approximate linear dependence of the gap on V_{SL}. Here, T is the total ramp time, and ν the ramp speed. While the energy gap for $V_{\mathrm{SL}} \to 0$ can become small for large system sizes, a gap to higher excited states set by discretization of the Bloch band will always exist in finite systems. Adiabaticity will be determined by the rate at which the Hamiltonian is modified relative to the energy gap, and the key question is how slow this ramp should be in order to obtain the η condensate with high fidelity for realistic system sizes ~ 100 sites [15].

Fidelity measures.—We measure closeness of the final state $|\psi_f\rangle$ to the η condensate in two ways: (a) via the full many-body fidelity $\mathcal{F} \equiv |\langle\psi_f|\eta_N\rangle|^2$, and (b) via the similarity of characteristic correlation functions of $|\psi_f\rangle$ to those of the η state. Remarkably, we will show below that fidelities $\mathcal{F} \sim 1$ can be obtained for long ramps, despite the fact that this quantity is exponentially sensitive to the system size, due to the increase in the size of the many-body Hilbert space. Indeed, we note that in large systems, states close to $|\eta_N\rangle$ can have essentially the same physical character as the desired state, and the associated correlation functions may not be significantly changed by a few small defects in the state, even if $\mathcal{F}$ becomes small. We thus also consider the comparison between characteristic correlation functions for the final state and $|\eta_N\rangle$, which gives a measure that can be directly measured in experiments, and is not exponentially sensitive to the size of the system. In particular, we are interested in the pair momentum distribution $\mathcal{C}_k(t) \equiv \mathcal{C}_k^{|\psi(t)\rangle}$, which can be measured, e.g., by associating atoms in doubly occupied sites to molecules, and releasing them from the lattice to perform a time-of-flight measurement. This correlation function is strongly peaked for $|\eta_N\rangle$, reflecting the off-diagonal long-range order exhibited by the η condensate in any dimension, with the pairing correlator $C_{\mathbf{m},\mathbf{n}}^{|\eta_N\rangle} = \langle\eta_N|c_{\mathbf{m},\uparrow}^\dagger c_{\mathbf{m},\downarrow}^\dagger c_{\mathbf{n},\downarrow} c_{\mathbf{n},\uparrow}|\eta_N\rangle = I_{M,N} e^{i\pi(\mathbf{m}-\mathbf{n})/M}$ (if $\mathbf{m} \neq \mathbf{n}$), and $I_{M,N} \equiv N(M - N)/(M - 1)$. The pair momentum distribution is the Fourier transform of this quantity, $\mathcal{C}_{\mathbf{k}}^{|\eta_N\rangle} \equiv \sum_{\mathbf{m},\mathbf{n}} e^{i\mathbf{k}(\mathbf{m}-\mathbf{n})} C_{\mathbf{m},\mathbf{n}}^{|\eta_N\rangle} = I_{M,N}\delta_{\mathbf{k},\pm\pi/a}$ [see Fig. 2(b)]. We will also consider the total distribution distance $\mathcal{D}(t) \equiv 1 - \sum_{\mathbf{k}}|\mathcal{C}_{\mathbf{k}}(t) - \mathcal{C}_{\mathbf{k}}^{|\eta_N\rangle}|/\sum_{\mathbf{k}}|\mathcal{C}_{\mathbf{k}}(t) + \mathcal{C}_{\mathbf{k}}^{|\eta_N\rangle}|$.

Many-body fidelities.—In Fig. 3(a) we plot the fidelity $\mathcal{F}$ at the end of the ramp as a function of ramp time T for
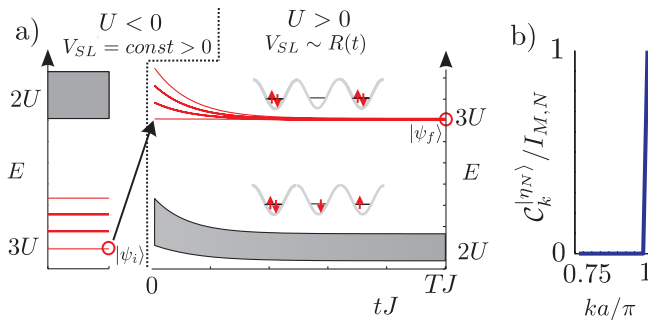
FIG. 2 (color online). (a) Energy eigenstates of $H_{\mathrm{FH}} + V$ as a function of time for a small example system with $N_\uparrow = N_\downarrow = 3$, $M = 6$. Left: Lowest energy states for strong initial attraction $U/J = -30$, in the presence of a superlattice. The lowest energy state is the initial state in our preparation scheme, $|\psi_i\rangle$. The shaded area denotes the excited manifold of states with one dissociated pair. Right: The highest energy levels of $H_{\mathrm{FH}} + V(t)$ as a function of time during the adiabatic ramp. The lowest energy eigenstate $|\psi(t)\rangle$ in the upper manifold where all atoms exist in pairs is equal to $|\eta_N\rangle$ at $t = T$. During the ramp, a gap of order U always exists to the manifold (shaded area) where some atoms are unpaired, and a gap to higher levels is present when the superlattice is present. (b) Pair momentum distribution $\mathcal{C}_k^{|\eta_N\rangle}$ of a perfect η condensate (see text).

different system sizes M. In order to perform more accurate calculations for reasonable computational time, these results are obtained in the limit $U \gg J$. Restricting to states that have only repulsively bound pairs, Hamiltonian (1) acts as [9] $H_S = -(J^2/U)\sum_{\langle i,j \rangle} \mathbf{S}_i \mathbf{S}_j + 2V_{\mathrm{SL}}\sum_{i \mathrm{even}} S_i^z$ in second order perturbation theory, with $\mathbf{S}_i = (S_i^x, S_i^y, S_i^z)$ denoting a vector of spin-1/2 operators, and spin states corresponding to sites that are occupied or unoccupied by a pair of atoms. Remarkably, for long ramp times it is possible to obtain unit fidelity, i.e., essentially perfect η condensates. The fidelities are also high for system sizes typical of current experiments, $M = 64$, and shorter time scales, $T \lesssim 1000J^{-1}$, which are realizable in current experiments. Although the time scales required to obtain a fixed fidelity increase with system size, we note (i) that we are already in the regime of experimentally relevant system sizes, and (ii) that the sensitivity of $\mathcal{F}$ increases exponentially with the size of the system, as discussed above.
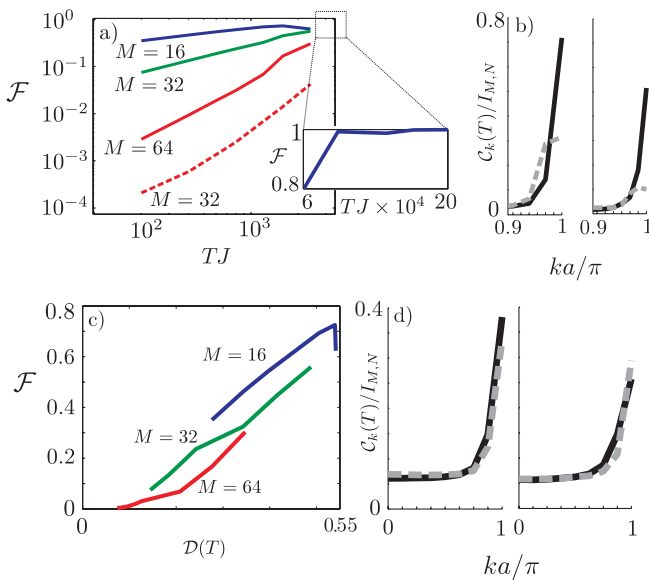

FIG. 3 (color online). (a) Fidelities for the superlattice and parabolic trap ramp as a function of ramp time T for different system sizes M, computed using H_S. The superlattice ramp shape is $V_{\mathrm{SL}} = 2J(e^{-\nu t} - e^{-\nu T})/(1 - e^{-\nu T})$, $\nu = J/8$. For the parabolic trap, we use the same shape with initial $V_P/J = 0.1$, $\nu = J/12$, and values for $M = 64$ are not shown as $\mathcal{F} \sim 10^{-12}$. U is decreased with the same shape as the potential in each case, with $U = 30J$ at $t = 0$, giving parameters for U and the superlattice that are typical of current experiments. The inset shows results for longer ramp times with $M = 16$. (b) On-site pair momentum distribution after $T = 2400J^{-1}$ for the superlattice (solid lines) and parabolic trap (dotted lines) ramps for $M = 32$ (left) and $M = 64$ (right), computed using H_S. (c) Final state fidelity $\mathcal{F}$ as a function of correlation function distance $\mathcal{D}(T)$ from the perfect η condensate, computed using H_S. (d) $\mathcal{C}_k(T)$ for superlattice ramps, computed using H_{FH}, with a number of impurities $N_i = 1$ (left) and $N_i = 2$ (right), for $T = 200J^{-1}$ (solid black lines), and $T = 400J^{-1}$ (grey dashed lines). The number of states retained in decompositions, $\chi = 200$ in (a–c), and $\chi = 400$ for (d).

Pair momentum distributions.—This picture is complemented by the pair momentum distributions, depicted in Fig. 3(b). In each case, the η-pairing peaks $\mathcal{C}_{\pi/a}$ are clearly visible, though for ramps with final fidelity lower than one, these peaks are somewhat broadened. In Fig. 3(c) we quantify this relationship between the fidelity $\mathcal{F}$ and the overlap of the pair momentum distribution with that of the perfect η condensate, as measured by $\mathcal{D}(T)$. Over a range of T values and system sizes these quantities are strongly correlated, so peak sharpness could be used to infer the quality of the η condensate in experiments.

Comparison with opening a harmonic trap.—For the same range of T and $M = 32, 48, 64$ we also compare our superlattice scheme to an adiabatic preparation scheme that was recently proposed, in which a band insulator is formed in the center of a harmonic trap $V_{\mathrm{trap}} \equiv \sum_i V_P(ia)^2$, and the trap is then opened to produce the final state [9]. As shown in Fig. 3(a), we see that for the same system sizes and ramping times, we obtain fidelities that are roughly 2 orders of magnitude smaller from ramping the harmonic trap. For $M > 32$, we see poorer scaling for the harmonic trap ramps than for the superlattice ramp (for 64 lattice sites we obtain fidelities $\mathcal{F} \sim 10^{-12}$). Similar effects are seen in Fig. 3(b) in the broadening of the final pair momentum distribution. In the superlattice scheme, mass is not redistributed across the whole system during the ramp, but instead global coherence is established via local interactions. In exact diagonalization with small systems, we correspondingly observe larger energy gaps for the superlattice as the additional potential is removed.

Imperfections.—We now investigate imperfections in the state preparation. First we address how missing atoms in the initial state, noise, and harmonic trapping potentials affect preparation of the η condensate. We then discuss how time-dependent measurement of correlation functions for the final state can be used to reveal and characterize these imperfections in experiments.

Imperfections—missing atoms.—To study the impact of missing atoms in the initial insulator state, we computed the time evolution of the adiabatic ramp (with the full Hamiltonian) starting with localized defects. Regardless of where these defects are present, and whether we have only missing atoms or complete missing pairs, this results in a broadening of the peaks in the pair momentum distribution. Examples are shown in Fig. 3(d) for a ramp at half filling with a number of missing atoms $N_i = 1, 2$. The resulting correlation functions are, however, stable in time (see below for further discussion).

Imperfections—noise.—Motivated by recent discussions [16], we also investigated this ramp in the presence of noise. This would primarily arise from fluctuations in the lattice depth, which would change the value of J. Note that in the superlattice ramp, J (coupling neighboring sites) is always nonzero, even though the effective tunneling at the beginning of the ramp is made small by the superlattice, $\sim J^2/\epsilon_{\mathrm{SL}}$. With a variation of J up to 10% with a variety of
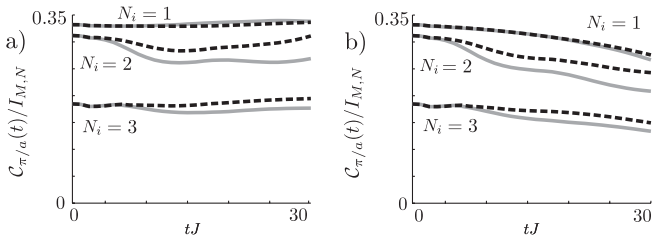
FIG. 4. Stability of a state close to an η condensate with imperfections. (a) Time dependence of $\mathcal{C}_{\pi/a}$ for the initial state with impurities as defined in the text on 32 sites, with 16 on-site pairs and varying impurity count N_i, for $U/J = 4$ (dashed black lines), $U/J = 10$ (solid grey lines). (b) Same as (a), but with additional trapping potential $V_P/J = 1.25 \times 10^{-4}$. The number of states retained in state decompositions, $\chi = 600$ in both parts.

correlation times for the noise, we found no significant effect on the final state fidelity.

Effect of a harmonic trap on preparation in a superlattice.—If a harmonic trap V_{trap} is present for the duration of the preparation, we find that the character of the final state in terms of the pair momentum distribution is close to the η condensate, though the peaks are slightly broadened and the density profile will correspond to a trap. This state is close to an excited eigenstate in the presence of the trap, and for $U \gg J$ is well approximated by an ansatz $\eta_{\mathbf{A}}^{\dagger} = \sum_i A_i c_{i,\uparrow}^{\dagger} c_{i,\downarrow}^{\dagger}$, where $\mathbf{A} \in \mathbb{R}^M$ correspond to the ground state wave function of a *single* bound particle with tunneling amplitude $-J^2/U$ in a trapping potential $2V_{\text{trap}}$.

Revealing and characterizing imperfections with an η condensate.—The η condensate is an exact excited eigenstate of the Fermi-Hubbard model, and the correlation functions will be both sharply peaked and stationary, unless there are errors in the state preparation or implementation of the Hamiltonian. Broadening and time dependence of the correlation functions can be used to reveal imperfections, and also to characterize their source. We consider an initial eta state, with N_i delocalized impurity atoms (see below for more details), and in Fig. 4 we plot the time dependence of the height of the peak in the pair momentum distribution. In Fig. 4(a) we consider only the additional atoms, and in Fig. 4(b) we add also a weak additional harmonic trapping potential. As in Fig. 3(d), increasing N_i reduces the height of the η-pairing peak. However, provided $U \gtrsim 4J$, the resulting pairs and the correlation functions are stable as a function of time. For $U < 4J$ (not shown) the pairs can decay through collision with unpaired atoms [4], and the peak in the pair momentum distribution also decays. On the other hand, additional potentials will dephase the state, and cause decay of the peak, as shown for a very weak harmonic trapping potential in Fig. 4(b). The rate of decay is larger for stronger traps due to faster dephasing, and unlike the effect of missing atoms, is independent of U/J. This difference could be used in an experiment to characterize the source of defects in the final state. Note that in order to make this

discussion independent of the form of the ramp, we have obtained the results in Fig. 4 beginning from a state of the form $|\eta, N, N_i\rangle \equiv \sum_{\{i\},\{j\}}: \prod_{n=1}^{N} (-1)^{i_n} \eta_{i_n}^{\dagger} \times \prod_{k=1}^{N_i} e^{i\delta j_k} c_{j_k,\downarrow}^{\dagger}: |0\rangle$ where $:\ldots:$ denotes the ordering operator by site, i.e., $: \eta_x^{\dagger} c_{y,\downarrow}^{\dagger} := \eta_x^{\dagger} c_{y,\downarrow}^{\dagger}$ if $x < y$ and $= c_{y,\downarrow}^{\dagger} \eta_x^{\dagger}$ otherwise. Note that $|\eta, N, N_i = 0\rangle = |\eta_N\rangle$.

Outlook.—The preparation of the η condensate offers a test bed to verify the emulation of many-body Hamiltonians in optical lattices, providing both a sensitive means to validate the implementation of the Hamiltonian, and also an important test case for state preparation schemes involving adiabatic ramps. These schemes are particularly important in light of the current experimental challenge to reduce entropies in order to generate states such as an antiferromagnetic phase of the Fermi-Hubbard model [17].

[1] M. Lewenstein *et al.*, Adv. Phys. **56**, 243 (2007); I. Bloch, J. Dalibard, and W. Zwerger, Rev. Mod. Phys. **80**, 885 (2008).
[2] R. Jördens *et al.*, Nature (London) **455**, 204 (2008); U. Schneider *et al.*, Science **322**, 1520 (2008); J. Mun *et al.*, Phys. Rev. Lett. **99**, 150604 (2007); S. Ospelkaus *et al.*, *ibid.* **96**, 180403 (2006).
[3] K. Winkler *et al.*, Nature (London) **441**, 853 (2006).
[4] N. Strohmaier *et al.*, Phys. Rev. Lett. **104**, 080401 (2010).
[5] C. N. Yang, Phys. Rev. Lett. **63**, 2144 (1989).
[6] E. Demler, W. Hanke, and S.-C. Zhang, Rev. Mod. Phys. **76**, 909 (2004).
[7] P. Rabl *et al.*, Phys. Rev. Lett. **91**, 110403 (2003).
[8] S. Trebst *et al.*, Phys. Rev. Lett. **96**, 250402 (2006); B. Paredes and I. Bloch, Phys. Rev. A **77**, 023603 (2008); J.-S. Bernier *et al.*, *ibid.* **79**, 061601(R) (2009); A. M. Rey *et al.*, Europhys. Lett. **87**, 60 001 (2009); A. S. Sorensen *et al.*, arXiv:0906.2567.
[9] A. Rosch *et al.*, Phys. Rev. Lett. **101**, 265301 (2008).
[10] U. Schollwoeck, Rev. Mod. Phys. **77**, 259 (2005); G. Vidal, Phys. Rev. Lett. **93**, 040502 (2004); S. R. White and A. E. Feiguin, *ibid.* **93**, 076401 (2004); A. J. Daley *et al.*, J. Stat. Mech. (2004) P04005.
[11] W. Hofstetter *et al.*, Phys. Rev. Lett. **89**, 220407 (2002).
[12] M. Popp *et al.*, New J. Phys. **8**, 164 (2006); A. Griessner *et al.*, *ibid.* **9**, 44 (2007).
[13] M. Anderlini *et al.*, Nature (London) **448**, 452 (2007); S. Trotzky *et al.*, Science **319**, 295 (2008).
[14] A. Borzi, G. Stadler, and U. Hohenester, Phys. Rev. A **66**, 053811 (2002).
[15] T. Rom *et al.*, Nature (London) **444**, 733 (2006).
[16] T. L. Ho (private communication).
[17] A. Koetsier *et al.*, Phys. Rev. A **77**, 023623 (2008).